DETACHED-EDDY SIMULATION: CURRENT STATUS AND PERSPECTIVES

Kyle D. Squires
MAE Department, Arizona State University, Tempe, AZ 85287-6106, U.S.A.
squires@asu.edu

Abstract Detached-Eddy Simulation (DES) is a hybrid technique proposed in 1997 as a numerically feasible and plausibly accurate approach for predicting massively separated flows. Since its inception the method has been applied to a range of configurations including simple shapes such as cylinders, spheres and aircraft forebodies, in addition to complex geometries including fighter aircraft. The accuracy of DES predictions has typically been far superior to that of steady or unsteady Reynolds-averaged Navier-Stokes methods while at the same time avoiding the Reynolds-number limitations that plague Large-Eddy Simulation. Based on research performed to date, the method appears sound and responds well to the type of boundary layer separation (i.e., laminar or turbulent), and to grid refinement. However, it is possible to degrade predictions using a grid density that is both too fine for RANS and too coarse for LES. Examples of applications of the technique are presented, along with a summary of some of the important findings and directions for future research.

Keywords: Turbulence simulation and modeling, hybrid methods, high Reynolds numbers

1. Introduction

Detached-Eddy Simulation (DES) is a hybrid technique first proposed by Spalart *et al.* (1997) for prediction of turbulent flows at high Reynolds numbers (see also Spalart 2000). Development of the technique was motivated by estimates which indicate that the computational costs of applying Large-Eddy Simulation (LES) to complete configurations such as an airplane, submarine, or road vehicle are prohibitive. The high cost of LES when applied to complete configurations at high Reynolds numbers arises because of the resolution required in the boundary layers, an issue that remains even with fully successful wall-layer modeling.

Traditionally, high Reynolds number separated flows have been predicted using solutions of the steady or unsteady Reynolds-averaged Navier-Stokes equations (RANS or URANS). One disadvantage of RANS methods applied to massive separations is that the statistical models are designed and calibrated on the basis of the mean parameters of thin turbulent shear flows containing numerous, and relatively "standard", eddies. Such eddies are not representative of the comparatively fewer and geometry-specific structures that typically characterize massively separated flows. The advantages then offered by LES provide strong motivation for its application, i.e., direct resolution of the dominant unsteady structures. In addition, while RANS or URANS does not appear to constitute a viable long-term approach for predicting massively separated flows at high Reynolds numbers, the calibration range of most models is sufficient to yield acceptable accuracy of a relatively broad range of attached flows. In Detached-Eddy Simulation (DES), the aim is to combine the most favorable aspects of the two techniques, i.e., application of RANS models for predicting the attached boundary layers and LES for resolution of time-dependent, three-dimensional large eddies. The cost scaling of the method is then favorable since LES is not applied to resolution of the relatively smaller-structures that populate the boundary layer.

In natural applications of the method, the entire boundary layer is treated by RANS and with an LES treatment of the separated regions. One of the issues confronting hybrid RANS-LES methods is the "grey area" in which a shear layer, after separation, must generate "LES content" (random eddies) which it did not possess in the boundary layer upstream. The process of generating LES content is more easily accommodated by a thin shear layer that is rapidly departing from the wall and for configurations with fixed separations (e.g., as occurs over geometries with sharp corners). In the examples summarized below, the challenge of separation prediction varies with the geometry and as will be shown, flow field predictions obtained using DES are encouraging. In the next section, an overview of the technique is presented, followed by a summary of some recent examples. A brief discussion then follows of some of the current issues requiring research in order to extend the range of applications amenable to accurate prediction using DES.

2. Detached-Eddy Simulation

The base model employed in the majority of DES applications to date is the Spalart-Allmaras one-equation model (Spalart and Allmaras 1994, referred to as "S-A" throughout). The reader is referred to Strelets (2001) for an analogous formulation based on the SST model. The S-A model contains a destruction term for its eddy viscosity $\tilde{\nu}$ which is proportional to $(\tilde{\nu}/d)^2$, where d is the distance to the wall. When balanced with the production term, this term adjusts the eddy viscosity to scale with the local deformation rate S and d: $\tilde{\nu} \propto Sd^2$. Subgrid-scale (SGS) eddy viscosities scale with S and the grid spacing Δ, i.e., $\nu_{SGS} \propto S\Delta^2$. A subgrid-scale model within the S-A formulation can then be obtained by replacing d with a length scale Δ directly proportional to the grid spacing.

To obtain the model used in the DES formulation, the length scale of the S-A destruction term is modified to be the minimum of the distance to the closest wall and a lengthscale proportional to the local grid spacing, i.e., $\tilde{d} \equiv \min(d, C_{DES}\Delta)$. In RANS predictions of high Reynolds number flows the wall-parallel (streamwise and spanwise) spacings are usually on the order of the boundary layer thickness and larger than the wall-normal spacing. Choosing the lengthscale Δ for DES based on the largest local grid spacing (i.e., one of the wall-parallel directions) then ensures that RANS treatment is retained within the boundary layer, i.e., near solid walls, $d << \Delta$ and the model acts as S-A, while away from walls where $\Delta << d$ a subgrid model is obtained.

There are several advantages to the DES formulation described above. The technique is non-zonal and simple in formulation, the transition between RANS and LES is seamless in that there is a single equation with no explicit declaration of RANS versus LES zones. The formulation using a single model only leads to a discontinuity in the gradient of the length scale that enters the destruction term of the turbulence model (this discontinuity would be easily removed by rounding the min function that determines the lengthscale). The change in the lengthscale leads to a model that becomes region-dependent in nature – in most cases a RANS model in the boundary layers and a subgrid model in separated regions. Incorporation of the grid spacing into the model is compatible with the existence of a filter width in LES that controls the end of the energy cascade. Grid refinement then provides a means to increase the range of scales and improve the fidelity of the calculation. This feature is quite unlike the role of grid refinement in RANS in which the role of the turbulence model remains important even in the fine-grid limit. While a natural choice, and an aspect of nearly all hybrid methods, incorporating the grid spacing into the model highlights the importance of grid design for any turbulence-resolving simulation technique. In boundary layers, as the grid spacing in the wall-parallel directions becomes smaller than about half of the boundary-layer thickness, the DES limiter reduces the eddy viscosity below its RANS level, though without allowing LES behavior. The resulting solution creates insufficient total Reynolds stresses, an issue that was raised in the original paper presenting the method by Spalart *et al.* (1997).

3. Applications

The DES applications summarized in this section are "natural" in the sense that boundary layers upstream of separation are handled by the RANS model, with the "LES region" comprising the detached regions away from the wall. The configurations include the flow over a sphere, around an aircraft forebody, and over fighter aircraft. With the exception of the sphere, all of the computations summarized in this manuscript were performed using the commercial flow solver *Cobalt*. The examples presented are representative of the variation in geometric complexity in research efforts undertaken to date and highlight the advantages of hybrid methods in general, and DES in particular, for prediction of high Reynolds number turbulent flows.

3.1 Turbulent Flow over a Sphere

The sphere belongs to the class of separated flows for which the location of flow detachment is not fixed by the geometry nor subject to external effects which might otherwise determine the location of boundary layer separation and/or force unsteadiness. These features in turn supply strong motivation for application of DES in order to assess both the strengths and limitations of the method.

As also the case for the circular cylinder, the sphere is known for its drag crisis, which reflects the substantial differences in separation between laminar and turbulent boundary layers. An illustration is provided in Figure 1, which shows contours of the instantaneous vorticity obtained from DES predictions of the sub-critical flow at $Re = 10^4$ (Constantinescu *et al.* 2003) and super-critical flow at $Re = 1.14 \times 10^6$ (Constantinescu *et al.* 2002). At $Re = 10^4$, the DES prediction is of a laminar boundary layer separation at an azimuthal angle measured from the forward stagnation point of around $82°$, in good agreement with experimental measurements (Achenbach 1972). The super-critical solution at $Re = 1.14 \times 10^6$ shown in the right frame of the figure experiences turbulent boundary layer separation at an azimuthal angle around $120°$, the DES prediction of the separation location also in good agreement with the experimental measurements reported by Achenbach (1972). Both frames in Figure 1 show a range of eddies that are resolved to the grid scale, the chaotic structure a result of the LES treatment in the wake.

The DES prediction of the laminar boundary layer separation in the sub-critical solution of the sphere is essentially a Large-Eddy Simulation, with the subgrid eddy viscosity predicted from a one-equation model (the S-A model modified in its destruction term). The non-trivial requirement that the turbulence model remains dormant in the laminar regions of the flow is achieved using the Spalart-Allmaras model. For the sub-critical flow over the sphere in Figure 1, the simulation is performed using the "tripless" approach proposed by Travin *et al.* (2000), which has the effect of disabling the model up to separation.

The solution for the high Reynolds number sphere shown in Figure 1 is of the fully turbulent flow modeled by seeding a small level of eddy viscosity into the domain upstream of the sphere, sufficient to ignite the turbulence

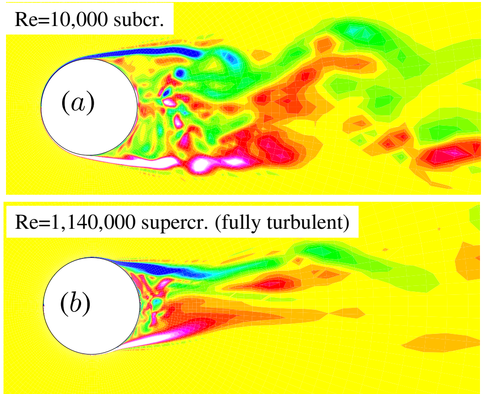

Figure 1. Contours of the instantaneous out-of-plane vorticity from DES predictions of the flow over a sphere. (a) sub-critical solution at $Re = 10^4$ with laminar boundary layer separation; (b) super-critical flow experiencing turbulent boundary layer separation at $Re = 1.14 \times 10^6$.

model as the fluid enters the boundary layers. Compared to the prediction at the lower Reynolds number, the fully turbulent treatment of the solution yields marked changes in the flow structure, with flow detachment substantially further aft compared to the laminar separation case. As also shown by Constantinescu *et al.* (2003), there are substantial differences between DES and URANS predictions of the time-dependent features of the solutions, with the URANS suppressing the development of turbulent eddies, reducing the three-dimensionality of the flow, and yielding essentially steady and axisymmetric solutions.

Prediction of flows experiencing turbulent boundary layer separation increase the burden on the model in predicting boundary layer growth and separation, now under control of a RANS model in DES. This increase in the empirical content of the approach is not inconsequential – essentially the entire boundary layer must be treated by RANS in applications and therefore the “RANS region” can substantially influence the overall accuracy of the prediction. The larger empirical input seems unavoidable at present since LES of the boundary layer, even with wall-layer modeling, is cost-prohibitive for full configurations.

A comparison of the pressure distributions to experimental measurements is shown in Figure 2. The DES prediction of the sub-critical flow at a Reynolds number of $Re = 10^5$ is in good agreement with the measurements of Achenbach (1972), the figure shows that the value and angular position of the minimum in C_p is recovered. For both the sub- and super-critical solutions the back

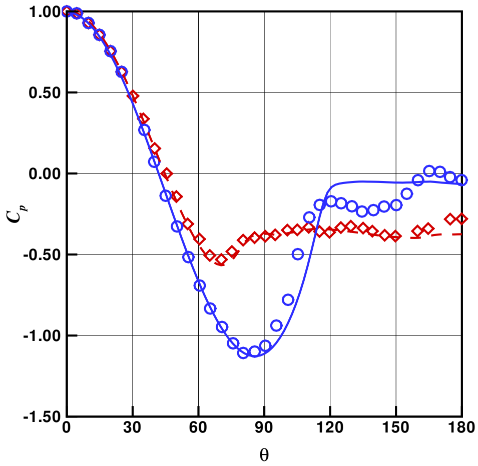

Figure 2. Pressure coefficient (averaged over the azimuthal coordinate). DES: ---- $Re = 10^5$; ——— $Re = 1.14 \times 10^6$. Achenbach (1972): $\diamond$ $Re = 1.62 \times 10^5$; $\circ$ $Re = 1.14 \times 10^6$.

pressure (at $\theta = 180°$) is also reasonably accurate, in turn yielding relatively accurate predictions of the drag. The figure is further useful for reinforcing the importance of the boundary layer treatment. In the super-critical regime, the delay in flow detachment substantially deepens C_p compared to the laminar separation solution. The fully turbulent DES predictions are, overall, in good agreement with the measurements. A difference compared to the sub-critical flow ($Re = 1.62 \times 10^5$) in the experiments is the greater variation in the pressure downstream of separation, an effect not produced in the simulations.

As also the case for the circular cylinder, even in the super-critical regime there are possibly substantial regions of the sphere in which the attached boundary layer is laminar. The details of flow separation and transition in the flow over the sphere are complex and the fully turbulent treatment summarized above is simplistic. A consequence of the simple, but well-defined, treatment of the boundary layers in the super-critical regime leads to relatively large discrepancies between the predicted and measured skin friction as shown in Constantinescu *et al.* (2002).

3.2 Flow around an Aircraft Forebody

The second example that represents an increase in geometric complexity compared to the sphere is the model of an aircraft forebody (Figure 3). Part of the motivation for the interest in the aerodynamics of such configurations is supplied by considerations of stability and control of aircraft at high angle of

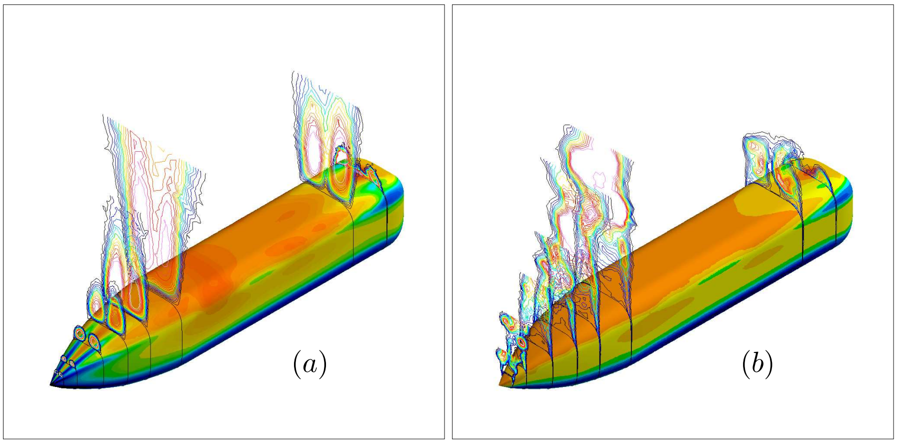

Figure 3. Ratio of the instantaneous eddy viscosity to the molecular value at eight axial locations for which pressure distributions are measured. Angle of attack of the freestream $\alpha = 90^\circ$, $Re = 2.1 \times 10^6$. (a) URANS; (b) DES. Surface colored by pressure.

attack. The unsteady separated flow around the forebody exerts considerable leverage, especially on modern fighter aircraft for which the forebody represents a relatively long moment arm.

The particular configuration described here was reported by Viswanathan *et al.* (2003) – a rectangular ogive forebody for which the length of the aft section is four times the width ("diameter", D), the cross-section being a rounded square in which the corner radius is 1/4 of the width and with a hemispherical end cap. Computations were performed at the highest Reynolds number for which measurements are available, $Re = 2.1 \times 10^6$ (based on freestream speed and diameter). Such a choice not only simplifies the simulation design in that predictions of the fully turbulent flow are a useful approximation to the experimental conditions, a more significant advantage is that the Reynolds number is representative of realistic flight configurations.

Shown in Figure 3 are contours of the eddy viscosity ratio along the ogive at the eight axial stations for which pressure measurements are available for assessing simulation results. DES predictions and URANS results obtained using the S-A model are shown for the freestream flow at angle of attack $\alpha = 90^\circ$. On the lee side, the URANS prediction shows that the wake is comprised of a pair of counter-rotating coherent vortical motions, as evidenced by the contours of the eddy viscosity in the planes and the signature of these structures on the surface pressure, especially along the forebody. The DES prediction, on the other hand, exhibits a more chaotic structure in the corresponding planes. Also apparent is the more uniform pressure on the leeward surface of the forebody, the figure showing a marked difference compared to the URANS result.

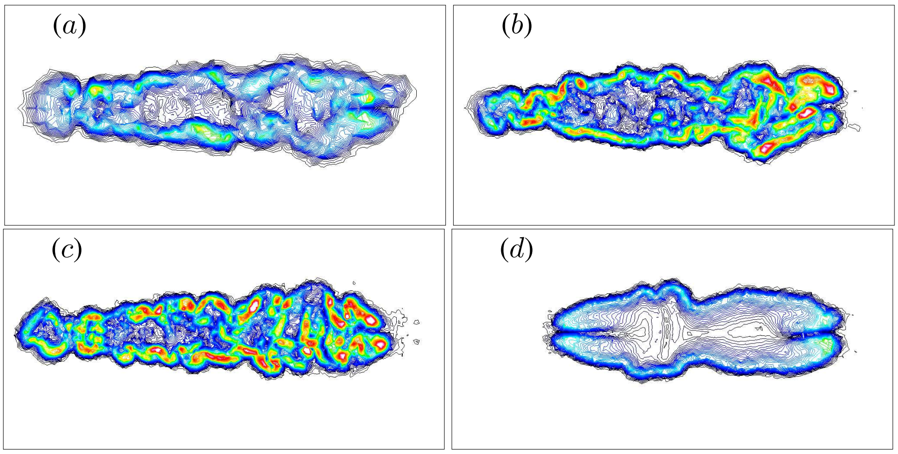

Figure 4. Contours of the instantaneous vorticity magnitude in the plane $y = D$, view is towards the freestream velocity. (a) coarse grid of 2.1×10^6 cells; (b) baseline grid of 6.5×10^6 cells; (c) fine grid of 8.75×10^6 cells; (d) URANS prediction on baseline grid.

A view of the influence of mesh refinement within DES is provided in Figure 4 in which contours of the instantaneous vorticity magnitude are shown in a plane normal to the freestream flow, in the wake of the ogive one-half diameter downstream of the rear surface. Calculations of the flow around the ogive were performed using unstructured grids, enabling a uniform refinement that was applied along each coordinate direction and with the corresponding grid sizes ranging from 2.1×10^6 to 8.75×10^6 cells. The DES predictions in the figure show a tapering of the wake towards the forebody. Figure 4 also shows that with increases in mesh resolution a wider range of scales is resolved, with substantial variation along the axial ("spanwise") coordinate.

A comparison of the pressure distribution predicted at the fourth axial station from the forebody nose (c.f., Figure 3) using DES and S-A URANS to the experimental measurements of Pauley *et al.* (1995) are shown in Figures 5. The angle θ is measured positive in the clockwise direction with $\theta = 0$ corresponding to the windward symmetry plane. As shown in the figure, the strong coherent vortices predicted in the RANS solution correspond to a large variation in pressure on the leeward side that differs markedly from the experimental measurements. The DES prediction of the pressure coefficient, on the other hand, is in excellent agreement with the measurements, a result of the more accurate resolution of the unsteady shedding that yields a uniform pressure profile on the leeward side.

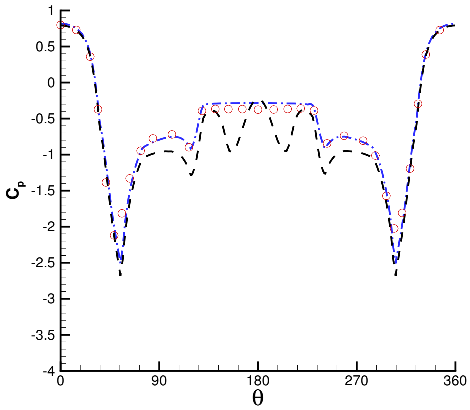

Figure 5. Pressure coefficient at $x/L = 0.166$ (fourth axial station from the nose), $Re = 2.1 \times 10^6$. DES: —·— ; URANS: - - - - ; Pauley *e*t al. (1995): ○ .

3.3 Flow around fighter aircraft

3.3.1 F-15E at 65 degrees angle of attack. Forsythe *et al.* (2003) have recently reported DES predictions of the flow over an F-15E at $\alpha = 65°$. An extensive flight-test database has been compiled on the F-15E that comprised the primary means of assessing DES predictions. The simulations were performed at standard day conditions corresponding to a chord-based Reynolds number of 13.6×10^6 and Mach number of 0.1. The investigation reported by Forsythe *et al.* (2003) was relatively comprehensive, examining sensitivity of DES predictions to mesh and timestep refinement, in addition to a comparison against RANS results obtained using the Spalart-Allmaras model.

Shown in Figure 6 is an isosurface of the instantaneous vorticity magnitude. The shear layer development off the leading edge of the wings is apparent in Figure 6, the LES treatment in the wake allows the development of an array of eddies. The computations reported by Forsythe *et al.* (2003) were performed on unstructured grids and with uniform mesh refinement along each coordinate direction. Contours of the instantaneous vorticity magnitude are shown in Figure 7 in a plane 680 inches aft of the aircraft reference point. As also observed for the geometrically-simpler forebody described above, a wider range of scales is captured with mesh refinement. The figure also shows that even the coarse grid comprised of 2.85×10^6 elements resolves at least some eddy content – with a few small structures visible above the wing.

Forsythe *et al.* (2003) found that DES predictions of the lift and drag were within 5% of flight-test data. Such predictions should be considered excellent, even once it is recognized that at $\alpha = 65°$, separation prediction is less chal-

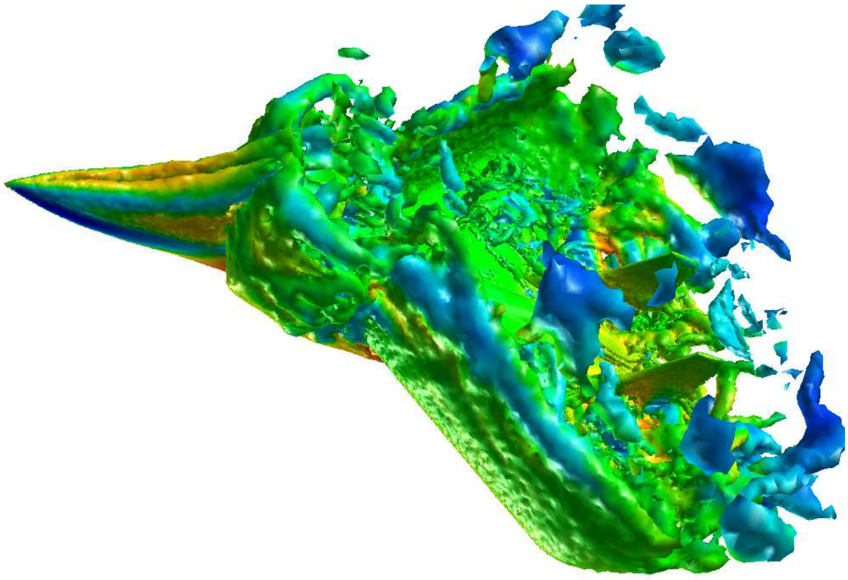

Figure 6. Isosurface of the instantaneous vorticity over the F-15E at 65° angle of attack.

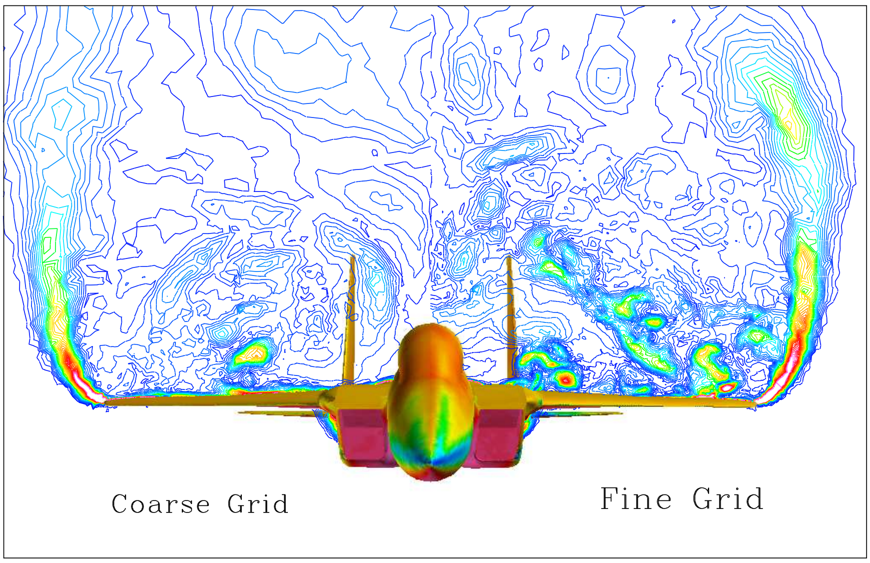

Figure 7. Contours of the instantaneous vorticity magnitude at 680 inches behind the aircraft reference point. Left frame: coarse grid comprised of 2.85×10^6 cells. Right frame: fine grid comprised of 10.0×10^6 cells. Aircraft surface colored by pressure.

lenging than at lower angles of attack and the success of DES can be attributed to its LES treatment of the separated regions. In the F-15E, regions of the flow over the aircraft such as the forebody were not resolved as well as in the component study reported by Viswanathan *et al.* (2003) and summarized above. Accommodating a resolution of the forebody comparable to that employed by Viswanathan *et al.* (2003) while also including the entire aircraft remains very challenging.

3.3.2 Abrupt wing stall over the F-18E. Forsythe and Woodson (2003) have recently reported DES and RANS predictions of the shock-separated flow over the F/A-18E. The work was motivated by the fact that during the envelope expansion flights of the F/A-18E/F, the aircraft encountered "wing drop", an event traced to an abrupt wing stall on either the left or right wing panel, causing a sudden and severe roll-off in the direction of the stalled wing. The phenomena is complex, measurements on a model of a pre-production F/A-18E reported by Schuster and Byrd (2003) showed that the surface pressure variations were highly unsteady and indicative of shock oscillation.

Shown in Figure 8a are time-averaged lift coefficients as a function of angle of attack. The predictions are obtained from a model of a pre-production F/A-18E with 10°/10°/5° flaps (leading-edge flaps/trailing-edge flaps/aileron flaps) at Mach 0.9 and without tails. DES predictions from a baseline and adaptively refined grid are shown, along with experimental measurements and RANS predictions. Figure 8a shows that the DES prediction on the baseline grid follows the lift curve to 9° angle of attack and with a subsequent decrease in the lift relative to the measured values. Using the adaptively refined grid, the DES predictions in the figure exhibit an improved agreement between simulation and experiment. Neither of the RANS results shown in Figure 8a follows the measured lift as closely as the DES predictions.

Shown in Figure 8b is a visualization of the instantaneous vorticity for the aircraft at 9° angle of attack. Unsteady pressure measurements show that the average pressure distribution is a result of an unsteady shock traveling forward and backward over the wing (Schuster and Byrd 2003). Forsythe and Woodson (2003) show that DES predictions exhibit a similar unsteady shock motion, the asymmetry in the flow structure in Figure 8b is a result of the unsteady shock motion, an effect that leads to large-magnitude low-frequency oscillations in the rolling moment. This inherently unsteady effect is captured in the DES, the work also showed that unsteady shock oscillations are a potential trigger event for abrupt wing stall.

3.3.3 Vortex burst over the F-18C. Morton *et al.* (2003) applied DES to prediction of the flow over an F-18C at $\alpha = 30°$. Part of the motivation for the work is the fact that the F-18 utilizes wing leading edge extensions to

(*a*)

(*b*)

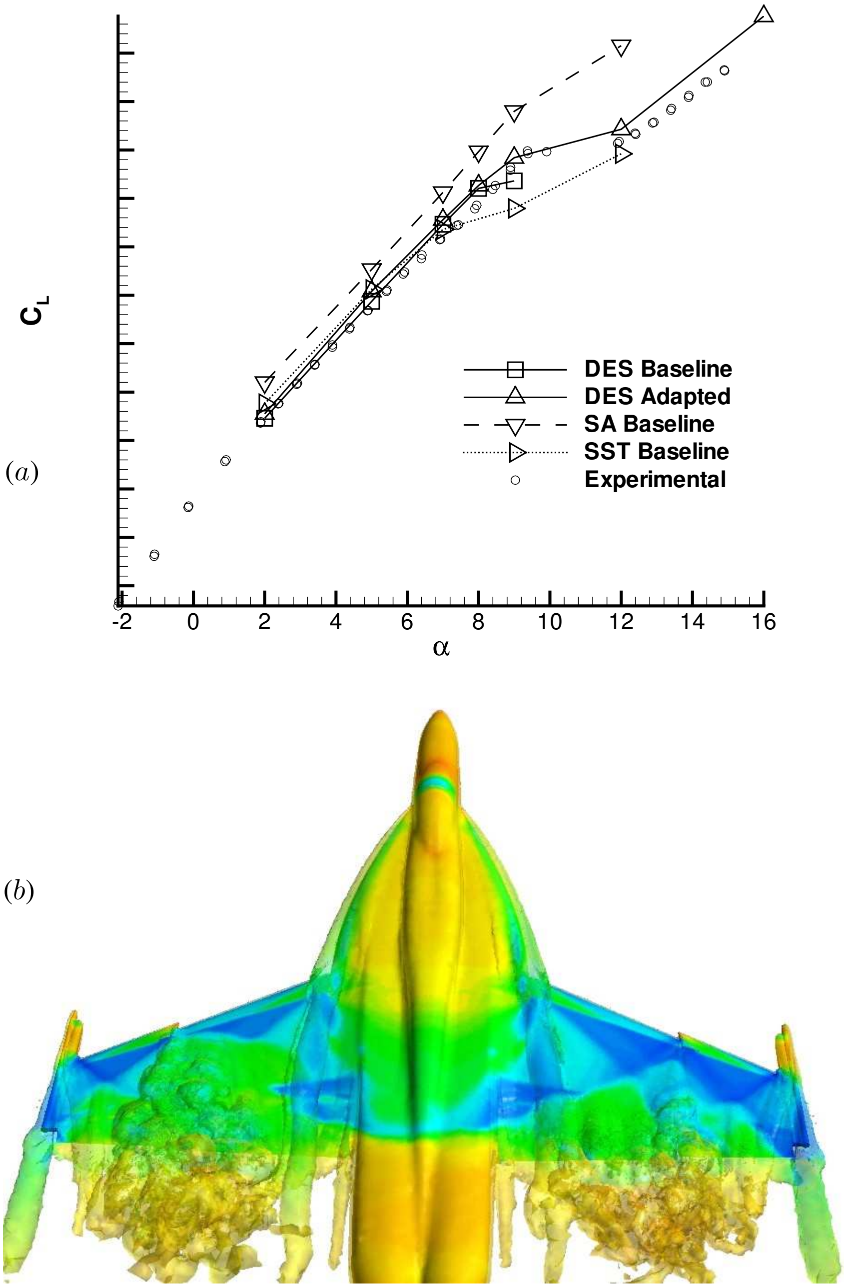

Figure 8. (*a*) Lift coefficient vs. alpha for the no tails F/A-18E. (*b*) Instantaneous isosurface of vorticity colored by pressure on the F/A-18E at 9° angle of attack.

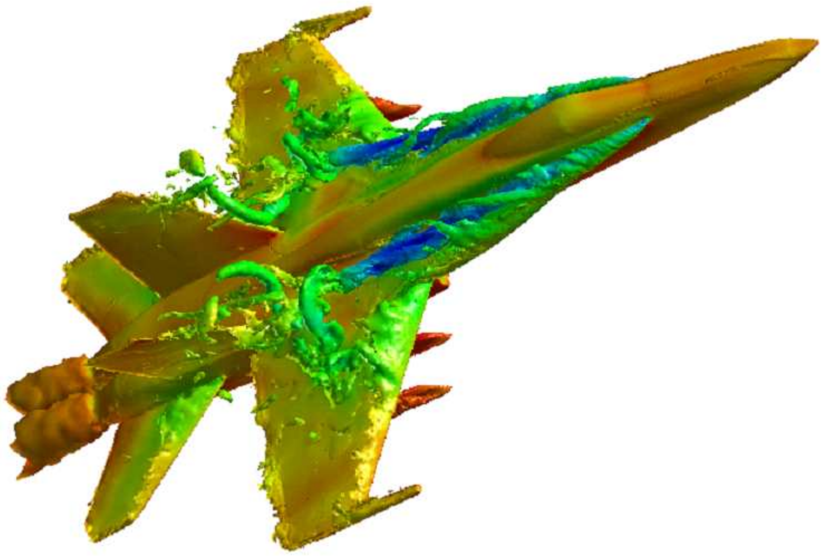

Figure 9. Isosurface of the instantaneous vorticity over the F-18C at 30° angle of attack.

generate vortices which enhance the wing lift and with the twin vertical tails canted in order to intercept the strong vortex field and increase maneuverability. At large angle of attack, these vortices break down upstream of the vertical tails, resulting in a loss of yaw control and severe aeroelastic effects. The flow field is inherently unsteady and requires an accurate prediction of vortex breakdown. These and other aspects challenge prediction and the flow appears to be well outside the boundaries of accurate prediction by RANS or URANS techniques.

The simulations reported in Morton *et al.* (2003) were performed at a chord-based Reynolds number of 13.9×10^6 and Mach number of 0.28. The work also provided an opportunity to apply and assess an important technology for eddy-resolving simulation of full aircraft – Adaptive Mesh Refinement. Shown in Figure 9 is an isosurface of the instantaneous vorticity magnitude. The development of the leading-edge extension vortex is apparent, also captured are smaller-scale structures that develop around the vortex. Figure 9 also shows that vortex breakdown occurs over the wing, as observed in flight and tunnel tests at $\alpha = 30°$. Morton *et al.* (2003) found that the DES prediction of the location of vortex breakdown was slightly aft of that observed in flight and tunnel tests at $\alpha = 30°$, though the differences compared to measurements were due to changes in the configuration considered in the calculations.

4. Summary

The examples summarized above highlight the strengths of the method, including a rational treatment of the attached boundary layers and the LES capability of the technique in separated regions. In massively separated flows, the demarcation between the RANS and LES regions is clear – a RANS model is applied to prediction of the attached boundary layer, new instabilities result in a rapid development of eddy structure in the wake that comprises the LES region. The eddy content evolves rapidly in the wake, the direct resolution of the energy-containing structures improves the visual description of the solutions and, more importantly, the quantitative prediction of, for example, the pressure distribution and forces and moments.

As true for any simulation technique that directly resolves turbulent eddies, and especially for applications aimed at complex geometries, grid design and construction is crucial to the overall success of the simulation. The reader is referred to Spalart (2001) for a guide on construction of DES grids. Grid adaption continues to evolve as a useful tool, the use of mesh adaption currently relies strongly on user guidance and therefore the need for expert users remains. Nevertheless, the developing experience base from DES applications considered to date make much more probable the success of multi-disciplinary efforts in areas such as aero-acoustics and fluid-structure interaction where accurate prediction of unsteady and three-dimensional turbulent eddies are required. Application of DES to these and other areas will further stress numerical treatments, requiring high fidelity from the underlying numerical schemes, among other factors.

For application of DES beyond regimes for which it was originally intended, e.g., to attached flows or flows exhibiting shallow separations, the influence of the "grey area" between the RANS and LES regions is more significant. An investigation relevant in this regard is that reported by Nikitin *et al.* (2000), in which DES was applied "as is", i.e., without any adjustment to the model, to turbulent channel flow. One of the goals of the investigation was to assess the method outside the original design range of massively separated flows. The channel flows in Nikitin *et al.* (2000) possessed sufficient wall-parallel grid spacings to resolve turbulent fluctuations in the core of the channel, not near the walls. Logarithmic velocity profiles were established in the RANS and LES regions, but with a "buffer layer" between the two regions in the vicinity of the RANS-LES interface and under-predictions in the skin friction of $\mathcal{O}(15)$ percent. Recently, it has been shown that stochastic forcing added to the momentum equations, accounting for backscatter of energy from the modeled to the resolved scales, can eliminate this mismatch (Piomelli *et al.* 2003). While the method outlined in Piomelli *et al.* (2003) is heuristic and introduced new parameters that are not preferable in routine applications, the findings are encouraging and motivate attempts at generalizing the approach.

Extension of DES to a wider range of flows will continue to motivate improvements in physical modeling and numerical aspects related to solution of the Navier-Stokes equations. Candidate flows include those exhibiting shallow separations and reattaching boundary layers, one motivating factor being the uneven performance of RANS models in predicting these flows. In these regimes, LES treatment within the boundary layer is attractive since it is possible to exploit the accuracy of the technique and grid-refinement possibilities inherent to the method – a proposition that is expensive, but will be useful and necessary for some applications.

Acknowledgments

This manuscript reflects substantial input and thoughtful comments over a range of DES research projects undertaken with Dr. Philippe Spalart, Dr. Jim Forsythe, and Dr. Scott Morton. The financial support of the Air Force Office of Scientific Research (Program Managers: Dr. Thomas Beutner and Dr. John Schmisseur), Office of Naval Research (Program Managers: Dr. Patrick Purtell and Dr. Ronald Joslin) and NAVAIR (Program Manager: Dr. Shawn Woodson) is gratefully acknowledged.

References

[1] Achenbach E.: *Experiments on the flow past spheres at very high Reynolds numbers*, J. Fluids Mech., **54**, pp. 565-575, (1972).

[2] Constantinescu G., Pacheco R., Squires K.D.: *Detached-Eddy Simulation of flow over a sphere*, AIAA Paper 2002-0425, (2002).

[3] Constantinescu G., Chapelet M., Squires K.D.: *On turbulence modeling applied to flow over a sphere*, AIAA Journal, **41**, pp. 1733-1742, (2003).

[4] Forsythe, J.R., Woodson, S.H.: *Unsteady CFD calculations of abrupt wing stall using Detached-Eddy Simulation*, AIAA Paper 2003-0594 (accepted for publication in AIAA Journal of Aircraft), (2003).

[5] Forsythe J.R., Squires K.D., Wurtzler K.E., Spalart P.R.: *Detached-eddy simulation of the F-15E at high alpha*, AIAA Journal of Aircraft, **40**, (2003).

[6] Morton S.A., Steenman M.B., Cummings R.M., Forsythe J.R.: *DES grid resolution issues for vortical flows on a delta wing and an F-18C*, AIAA Paper 2003-1103, (2003).

[7] Nikitin N.V., Nicoud F., Wasistho B., Squires K.D., Spalart P.R.: *An approach to wall modeling in Large-Eddy Simulations*, Phys. Fluids **12**, pp. 7-10, (2000).

[8] Pauley, H., Ralston, J., Dickes, E.: *Experimental study of the effects of Reynolds number on high angle of attack aerodynamic characteristics of forebodies during rotary motion*, NASA CR 195033, (1995).

[9] Piomelli, U., Balaras, E., Pasinato, H., Squires, K.D., Spalart, P.R.: *The inner-outer layer interface in Large-Eddy Simulations with wall-layer models*, Int. J. Heat and Fluid Flow, **24**, pp. 538-550, (2003).

[10] Schuster, D., Byrd, J.: *Transonic unsteady aerodynamics of the F/A-18E at conditions promoting abrupt wing stall*, AIAA Paper 2003-0593, (2003).

[11] Spalart P.R.: *Strategies for turbulence modelling and simulations*, Int. J. Heat Fluid Flow, **21**, pp. 252-263, (2000).

[12] Spalart P.R.: *Young person's guide to Detached-Eddy Simulation grids*, NASA CR-2001-211032, (2001).

[13] Spalart, P.R., Allmaras, S.R.: *A one-equation turbulence model for aerodynamic flows*, La Recherche Aerospatiale, **1** pp. 5-21, (1994).

[14] Spalart P.R., Jou W.H., Strelets M., Allmaras S.R.: *Comments on the feasibility of LES for wings, and on a hybrid RANS/LES approach*, 1st AFOSR Int. Conf. on DNS/LES, Aug. 4-8, 1997, Ruston, LA. In: Advances in DNS/LES, C. Liu and Z. Liu Eds., Greyden Press, Columbus, OH, USA (1997).

[15] Strelets M.: *Detached eddy simulation of massively separated flows*, AIAA-2001-0879, (2001).

[16] Travin A., Shur M., Strelets M., Spalart P.R.: *Detached-Eddy Simulations past a Circular Cylinder*, Flow, Turb. Comb., **63**, pp. 293-313, (2000).

[17] Viswanathan, A., Squires, K.D., Forsythe, J.R.: *Detached-Eddy Simulation around a fore-body at high angle of attack*, AIAA Paper 2003-0263, (2003).